Dalton Transactions

ROYAL SOCIETY OF CHEMISTRY

PAPER

View Article Online
View Journal | View Issue

Cite this: *Dalton Trans.*, 2022, **51**, 9836

Covalent triflates as synthons for silolyl- and germolyl cations†

Wiebke Marie Wohltmann, Marc Schmidtmann and Thomas Müller *

Received 10th May 2022,
Accepted 9th June 2022

DOI: 10.1039/d2dt01446g

rsc.li/dalton

The synthesis of 1-silolyl and 1-germolyl triflates from the corresponding chlorides by salt metathesis reaction is reported. These covalent triflates are ideal starting materials for the preparation of ionic silolyl- and germolyl-imidazolium triflates by their reaction with N-heterocyclic carbenes. Similarly, ionic silolyl- and germolyl-oxophosphonium triflates are obtained by substitution of the triflate group by triethylphosphane oxide Et_3PO. The analysis of their ^{31}P NMR chemical shifts according to the Gutmann–Beckett method reveal the high Lewis acidity of the underlying silolyl and germolyl cations. Further analysis of structural and NMR parameters of the silolyl- and germolyl-imidazolium and oxophosphonium triflates indicates that these compounds are covalently bonded silole and germole derivatives with insignificant contributions from silolyl- or germolyl cations. Silolyl and germolyl triflates are however synthetic equivalents of these cations and might serve as a source for electrophilic silolyl and germolyl units.

Introduction

Sila- and germacyclopentadienes **1** (siloles and germoles) found widespread interest due to their favorable photophysical properties.[1–4] Cross hyperconjugation between the ER_2 group and the butadiene part of the heterocycle results in a substantial lowering of the LUMO and an increase of the electron affinity of the group 14 heteroles (tetroles).[5–8] In addition, the discovery of the aggregation induced emission (AIE) effect of aryl-substituted siloles by Tang and coworker provided a new impetus to this field and had significant impact on materials chemistry.[9–11] The interest of our group in silole and germole chemistry was directed to their use as starting materials for new silicon and germanium heterocycles with unprecedented structures and properties.[12] During these investigations, we studied the synthesis and properties of classical reactive intermediates such as the heterolyl radicals **2**, heterolyl anions **3** and of more uncommon intermediates such as heterolyl dianions **4** (Fig. 1).[13–16] The missing link in these series of reactive tetrolyl derivates are the corresponding cations **5**. Silolyl and germolyl cations **5** are isolobal to boroles[17–21] and alumoles[22–26] and therefore they are potentially antiaromatic species of high Lewis acidity. The Lewis acidity of these species should clearly exceed that of the neutral group 13 heterocyclopentadienes due to their extra positive charge and the expected lowering of their LUMO energy level. In view of the unprecedented reactivity of cationic[16] or electron deficient boroles, such as Piers' borole **6**,[27–31] we were convinced that these tetrolyl cations are rewarding synthetic targets.

We report here on our attempts to synthesize silolyl and germolyl cations and on our finding that covalent heterolyl triflates are ideal starting materials for the synthesis of ionic heterolyl triflates that allows gauging the Lewis acidity of the underlying cations.

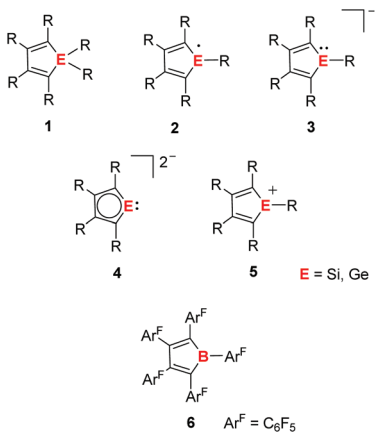

Fig. 1 Tetroles, tetrolyl radicals, anions, dianions, and cations and Piers' borole.

Institute of Chemistry, Carl von Ossietzky University Oldenburg, Carl von Ossietzky-Str. 9-11, 26129 Oldenburg, Germany.
E-mail: thomas.mueller@uni-oldenburg.de

†Electronic supplementary information (ESI) available: Experimental details, analytical data, complete XRD data and details of the computational work. CCDC 2170123–2170134. For ESI and crystallographic data in CIF or other electronic format see DOI: https://doi.org/10.1039/d2dt01446g

Results and discussion

Initially, we investigated tetrolyl cations $[7]^+$ and $[\mathbf{8a}]^+$ computationally and compared their structural and electronic properties with that of the isoelectronic borole **9** and alumole **10**.[32] We choose for this DFT study at the M06-2X/def2-TZVP-level a substitution pattern at the heterocyclopentadiene ring that is identical or close to that used in the experimental study.

Structure optimization of these four heterocyclopentadienes gave localized double and single bonds for the butadiene part of the heterole ring (Table 1). The inner-cyclic C–C bond lengths for all four compounds are remarkably similar and differ significantly from those calculated for the silole ($[\mathbf{11}]^{2-}$) and germole dianion ($[\mathbf{12}]^{2-}$), both with a delocalized 6π-electron system.[15] In agreement with these structural parameters, nucleus independent chemical shift (NICS) calculations, an established computational aromaticity/antiaromaticity test protocol,[33,34] suggest for both cations $[7]^+$ and $[\mathbf{8a}]^+$ as well as for the neutral borole **9** a marked antiaromatic character ($NICS(1)^{zz}$ = +21 to +25). The alumole **10** is according to the NICS-criteria less antiaromatic. For the dianions $[\mathbf{11}]^{2-}$ und $[\mathbf{12}]^{2-}$ strongly negative $NICS(1)^{zz}$ values indicate the aromatic ring current and serve here as example for aromatic heterole derivatives. The calculated shape of frontier orbitals for the heterocyclopentadienes $[7]^+$, $[\mathbf{8a}]^+$, **9** and **10** are all very similar: the HOMO being the non-symmetric combination of the two π–CC bonds and the LUMO being localized mainly at the heteroatom (see Fig. 2 for a representative example). As a result of the positive charge of the silicon and germanium species the LUMO energy levels for the tetrolyl cations are much lower than calculated for the neutral boron and aluminum heterocycles (Table 1). This implies high Lewis acidity for the cations, which is corroborated by very high calculated fluoride ion competition (FIC) energies ($[7]^+$: 453 kJ mol^{-1}; $[\mathbf{8a}]^+$, 353 kJ mol^{-1}, see Table 1).[35,36] The FIC energies were calculated using the pair $[FBEt_3]^-/BEt_3$ according to Scheme 1 and as cornerstones serve the FIC values of antimony pentafluoride (248 kJ mol^{-1}), of tris-pentafluorophenylborane (BCF, 155 kJ mol^{-1}) and of trimethylsilylium (462 kJ mol^{-1}).

The computational evaluation of tetrolyl cations $[7]^+$ and $[\mathbf{8a}]^+$ suggests that these cations are antiaromatic similar to the isoelectronic boroles. Due to their positive charge the LUMO energy level is however significantly lowered, which results in a very high predicted Lewis acidity.

In our hands, the established protocols for tetryl cation synthesis were unsuccessful for the preparation of silolyl and germolyl cations.[37] That is, the reaction of 1-hydrido-1*H*-germoles and 1*H*-siloles with trityl cation in the presence of a weakly coordinating anion (WCA) (Corey reaction, Scheme 2,

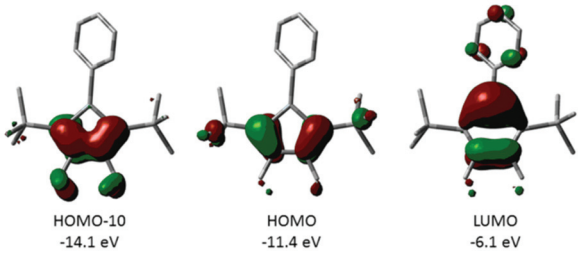

Fig. 2 Surface diagrams of the π-orbitals of germolyl cation $[\mathbf{8a}]^+$ (calculated at M062X/def2-TZVP for the isolated molecule, isodensity value 0.05).

Scheme 1 Fluoride ion competition [FIC] reaction to evaluate the acidity of different Lewis acids LA.[35,36]

Table 1 Computed bond lengths [pm], LUMO energies (eV), nucleus independent chemical shifts (NICS) and fluoride ion competition (FIC) values [kJ mol^{-1}] of heterolyl cations and related species (M06-2X/def2-TZVP)

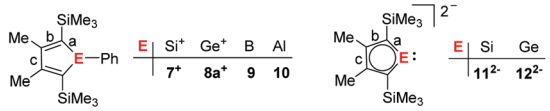

Cpd	*a* [pm]	*b* [pm]	*c* [pm]	NICS $(1)^{zz}$ [a]	*E*(LUMO) [eV]	FIC[b] [kJ mol^{-1}]
7^+	182	136	155	+21	−4.36	435
$\mathbf{8a}^+$	192	136	155	+21	−4.38	353
9	158	135	153	+25	−1.65	77
10	194	135	154	+12	−1.29	152
$\mathbf{11}^{2-}$	186	144	139	−18		
$\mathbf{12}^{2-}$	196	143	139	−19		

[a] $NICS(1)^{zz}$: Eigenvector of the NICS calculated for a point 100 pm above the center of the five-membered ring that is orthogonal to the ring plane. [b] FIC values and LUMO energy levels are calculated using the SCIPCM method to include the influence of the solvent benzene.

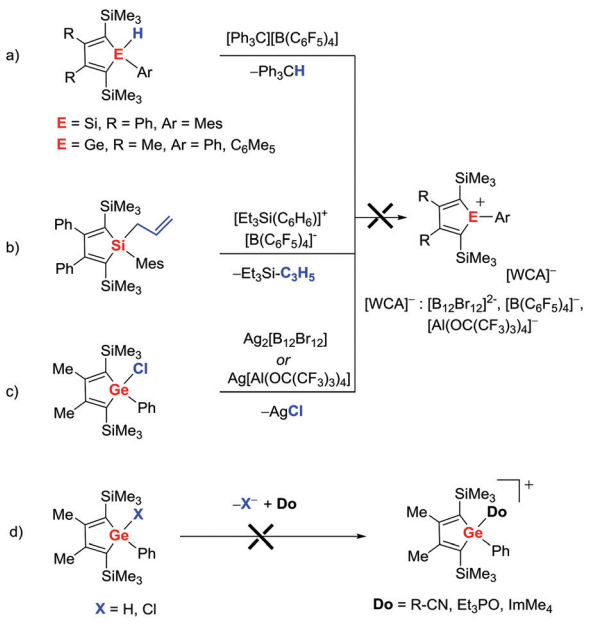

Scheme 2 Attempted synthesis of silolyl and germolyl cations.

path a)[38,39] failed in all investigated cases. Either the reaction was very slow (with large aryl groups) or it led to a mixture of non-identified compounds (with small aryl groups). Similarly, the method of Lambert and colleagues to apply an allyl unit as leaving group using triethylsilylbenzenium as electrophile failed (Scheme 2, path b).[40] The salt metathesis reaction using silver salts of WCAs is a viable route to germylium ions.[41,42] We observed, however, no reaction of a 1-*H*-germole chloride with silver salts of two different WCAs (Scheme 2, path c). Even in the presence of external donors with the potential to stabilize the incipient cation, the ionization of a 1-*H*-germole was not successful (Scheme 2, path d).

In contrast to silver salts of WCAs (Scheme 2, path c), silver triflate reacts in toluene at room temperature with 1*H*-germolyl and 1*H*-silolyl chlorides, **13** and **14**, to give the corresponding heterolyl triflates **15** and **16** in high isolated yields (74–92%, Scheme 3). While there is no reaction of chlorides **1** and **2** with the N-heterocyclic carbene 1,3,4,5-tetramethylimidazol-2-ylidene ($ImMe_4$), the corresponding triflates **15** and **16** undergo a clean substitution reaction to give the germolyl- and silolylimidazolium triflates **17**[OTf], **18**[OTf] in almost quantitative yields (see Scheme 3).

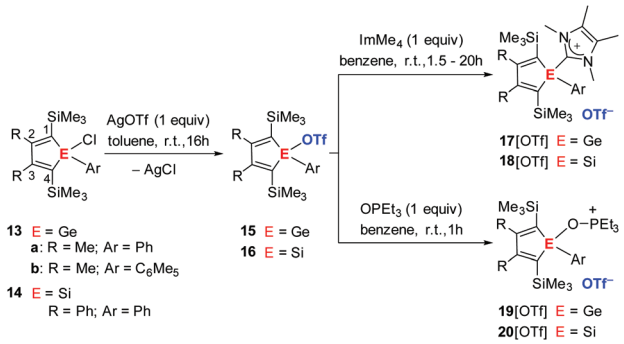

Scheme 3 Synthesis of tetrolyl triflates **15**, **16**, [**17**]–[**20**]OTf.

The newly synthesized compounds were characterized by multinuclear NMR spectroscopy and X-ray diffraction (XRD) analysis. The ^{13}C NMR chemical shifts of the ring carbon atoms C^1–C^4 of triflates **15**, **16**, **17**[OTf] and **18**[OTf] are unremarkable and differ only slightly from those of the corresponding chlorides (see Table 2). It is worth mentioning that the calculated ^{13}C NMR chemical shifts for DFT-optimized molecular structures of the investigated molecules and cations differ only slightly ($\Delta\delta^{13}C^{theo}$ = 0 to −5, Table 2). Compared to other silyltriflates (*e.g.* Me_3SiOTf, $\delta^{29}Si$ = 43.7),[37] the ^{29}Si NMR resonance of the covalent silolyl triflate **16** is high-field shifted and matches almost that of silolyl chloride **14**. The silicon nuclei of the ionic imidazolium triflate **18** is even stronger shielded (by $\Delta\delta^{29}Si$ = 22.8 compared to the triflate **16**) and indicates tetracoordination for the silole-silicon atom (see Table 2). The strong coordination of the carbene to the tetrole ring finds additional support by the high-field ^{13}C NMR resonance of the carbene carbon atom of the $ImMe_4$ substituent in triflates **17**[OTf] and **18**[OTf]. The ^{13}C NMR signals are shifted from $\delta^{13}C$ = 213.7 for $ImMe_4$ to a region that is typically found for silyl imidazolium ions ($\delta^{13}C$ = 144.2–146.4 ([**17**]$^+$, [**18**]$^+$) *vs.* $\delta^{13}C$ = 145 ([**21**]$^+$)).[43–47] The resonance frequencies of the ^{15}N nuclei vary only slightly compared to those of the free carbene ([**17**]$^+$, [**18**]$^+$: $\delta^{15}N$ = 180.9–184.9, $ImMe_4$: $\delta^{15}N$ = 177.5).[48] Interestingly, the ^{13}C NMR chemical shift of the CF_3 group of the covalently bound triflate group in **15** and **16** differs by $\Delta\delta^{13}C$ = 3 from those of the same group in the ionic imidazo-

Table 2 Experimental NMR data of silole and germole derivatives **13**–**16** and triflates **17**[OTf]–**20**[OTf]. Calculated NMR chemical shifts (in parenthesis, italic, at M06L/def2tzvp//M06-2X/def2-tzvp)

Cpd	$\delta^{13}C$(1/4)	$\delta^{13}C$(2/3)	$\delta^{29}Si$	Others[a]
13a	136.8	163.9		
13b	142.7	159.9		
14	140.0	171.6	17.9	
15a	131.5 (*128*)	167.4 (*165*)		$\delta^{13}C(CF_3)$ = 119.8
15b	136.2 (*133*)	164.4 (*162*)		$\delta^{13}C(CF_3)$ = 119.6
16	135.4	175.5	16.5	$\delta^{13}C(CF_3)$ = 119.3
17a[OTf]	137.4 (*130*)	166.5 (*167*)		$\delta^{13}C(NCN)$ = 144.1; $\delta^{13}C(CF_3)$ = 122.1; $\delta^{15}N$ = 182.3
17b[OTf]	140.8 (*135*)	165.0 (*165*)		$\delta^{13}C(NCN)$ = 148.3; $\delta^{13}C(CF_3)$ = 122.6; $\delta^{15}N$ = 180.9
18[OTf]	140.0	175.1	−6.3	$\delta^{13}C(NCN)$ = 141.9; $\delta^{13}C(CF_3)$ = 122.2; $\delta^{15}N$ = 184.9
19a[OTf]	131.3 (*128*)	169.0 (*168*)		$\delta^{13}C(CF_3)$ = 122.3; $\delta^{31}P$ = 93.2
19b[OTf]	137.1 (*133*)	166.2 (*164*)		$\delta^{13}C(CF_3)$ n.d.; $\delta^{31}P$ = 92.7
20[OTf]	136.1	175.1	9.6 ^2J(SiP) = 15 Hz	$\delta^{13}C(CF_3)$ = 121.8; $\delta^{31}P$ = 98.9
[**8a**]$^+$	(*119*)	(*181*)		
[**7**]$^+$	(*112*)	(*188*)	(*228*)	

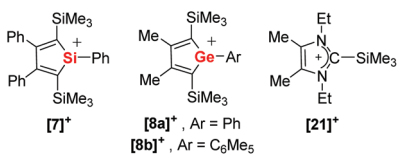

[a] ^{19}F NMR chemical shifts are given relative to $\delta^{19}F(CFCl_3)$ = 0; ^{15}N NMR chemical shifts are given relative to $\delta^{15}N(H_3CNO_2)$ = 379.9.

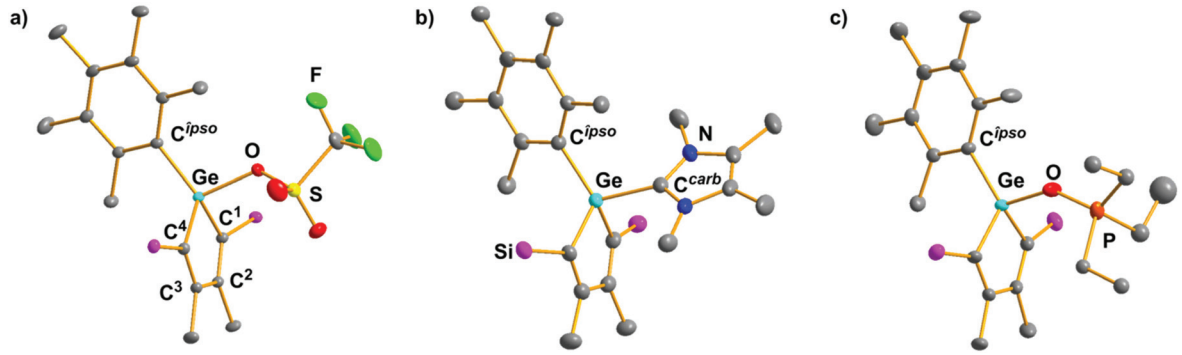

Fig. 3 Molecular structures (a) of germole triflate **15b** in the crystal; (b) of the cation [**17b**]$^+$ in the crystal **17b**[OTf]; (c) of the cation [**19b**]$^+$ in the crystal of **19b**[OTf]. Thermal ellipsoid presentation at 50% probability, hydrogen atoms and silyl methyl groups are omitted. Pertinent bond lengths [pm] and angles [°]. **15b**: Ge–C^1 193.60(12), Ge–C^4 193.92(12), C^1–C^2 136.02(15), C^2–C^3 151.76(17), C^3–C^4 135.33(15), Ge–C^{ipso} 194.62(10), Ge–O 191.23(8), $\sum\alpha(GeC_3)$ = 341.9. [**17b**]$^+$: Ge–C^1 196.13(25), Ge–C^4 194.85(26), C^1–C^2 135.31(37), C^2–C^3 150.51(35) C^3–C^4 135.29(37), Ge–C^{ipso} 196.16 (25), Ge–C^{carb} 200.90(26), $\sum\alpha(GeC_3)$ = 334.8. [**19b**]$^+$: Ge–C^1 194.39(18), Ge–C^4 193.80(19), C^1–C^2 135.48(29), C^2–C^3 152.58(28) C^3–C^4 135.47(28), Ge–C^{ipso} 195.35(18), Ge–O 185.13(15), O–P 154.47(16), α (Ge–O–P) 140.606(97), $\sum\alpha(GeC_3)$ = 337.5.

lium triflates **17**[OTf] and **18**[OTf]. Although the difference is small, it is reproducible and significant (Table 2). Given that the salt-like composition of **17**[OTf] and **18**[OTf] is demonstrated by its solid state structure (see below), this ^{13}C NMR chemical shift difference to the covalently bound sulfonylesters **15** and **16** indicate its ionic nature also in benzene solution. To summarize, our accumulated NMR data give no indication of a tetrolyl cation character of the investigated compounds. In particular, their experimental NMR data differs significantly from those calculated for germolyl cations [**8**]$^+$ and silolyl cations [**7**]$^+$ (see Table 2).

The solid-state structures of compounds **15**, **16** and **17**[OTf], **18**[OTf] could be resolved and their structural molecular parameters are given in the ESI.† Fig. 3 shows the molecular structures of the pentamethylphenyl substituted germolyl species **15b** and [**17b**]$^+$ and provides structural parameters that are representative for this class of compound. The central tetrolyl units of compounds **15**, **16** and **17**[OTf], **18**[OTf] closely resembles each other. All are almost planar, and the butadiene unit shows the expected bond length alternation (C^1=C^2/C^3=C^4: 135–136 pm; C^2–C^3: 151–153 pm). The inner cyclic Ge–C^1/C^4 bond lengths in the germole derivatives **15** and [**17**]$^+$ (193–196 pm) are at the shorter end of the typical range of Ge–C bonds (195–200 pm).[49] Similarly, the Si–C^1/C^4 bonds in siloles **16** and [**18**]$^+$ (185–187 pm) are slightly shorter than the standard value for Si–C(sp^2) bonds of 187.8 pm.[50] The E–O bonds of the covalent triflates **15** and **16** are longer than typical Ge–O (175–185 pm) or Si–O (162.9 pm) bonds.[49,50] Finally, the E–C^{carb} are in the typical range for NHC–carbon–germanium or –silicon bonds (200–205 pm).[51–53] The coordination environment of the silicon and the germanium atoms in **15**, **16**, [**17**]$^+$, and [**18**]$^+$ is tetrahedral, even the pentamethylphenyl-substituted germanium derivatives **15b** and [**17b**]$^+$ show no pronounced trigonal flattening. Taking the sum of the bond angles between the germanium atom and its three carbon substituents $\sum\alpha(GeC_3)$ as an indicator,[54,55] it is obvious that neither the triflate **15b** nor the germolylimidazolium cation [**17b**]$^+$ shows significant germylium ion-like character. Both their $\sum\alpha(GeC_3)$ values are far from 360°, the ideal value for germylium ions and are in the typical range of tetracoordinated germanium compounds (Fig. 4). In summary, also the structural data of triflates **15**, **16** and **17**[OTf], **18**[OTf] give no indication of tetrolyl cation character. This is in agreement with the substantial bond dissociation energy, BDE, that is calculated for the Si–C^{carb} and Ge–C^{carb} bonds in [**17**]$^+$ and [**18**]$^+$ (BDE = 327 ([**17a**]$^+$); 282 ([**17b**]$^+$); 350 ([**18**]$^+$) kJ mol^{-1}) and which are in the same

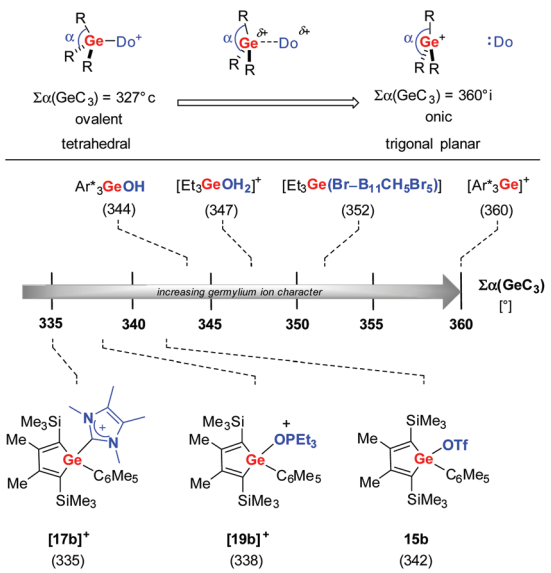

Fig. 4 Top: The sum of the bond angles of the GeR$_3$ group, $\sum\alpha(GeC_3)$, as a structural measure for the covalent character of the Ge–Do linkage (Do = donor).[54,55] Bottom: Sequence of $\sum\alpha(GeC_3)$ of representative examples for free germylium ions, donor-stabilized germylium ions and triaryl germanol Ar*$_3$GeOH (Ar* = 2,6-bis(*tert*-butoxyphenyl).[42,59,60] The data of the germolyl derivatives **15b**, [**17b**]$^+$ and [**19b**]$^+$ are shown for comparison.

order than typical bond strength of Ge–C (255 kJ mol^{-1}) and Si–C (301 kJ mol^{-1}) single bonds.[56–58]

Although the synthesis of salts of heterolyl cations [**7**]$^+$ and [**8**]$^+$ was not successful, we were able to determine their Lewis acidity by applying the Gutmann–Beckett protocol.[61,62] The covalent triflates **15** and **16** react readily with triethylphosphane oxide, Et_3PO, at room temperature in benzene to give the germolyl- and silolyl-oxyphosphonium triflates **19a**[OTf], **19b**[OTf] and **20**[OTf] in high isolated yields (68–98%; see Scheme 3). All three oxophosphonium triflates were fully characterized by NMR spectroscopy and XRD analysis. The obtained ^{31}P NMR data characterize all three investigated cations as strong Lewis acids (see Table 2). The determined deshielding relative to Et_3PO, $\Delta\delta^{31}$P, indicates that the germolyl cations [**8**]$^+$ ($\Delta\delta^{31}$P = 46.5–47.0) and the silolyl cation [**7**]$^+$ ($\Delta\delta^{31}$P = 52.7) are stronger Lewis acids than the isoelectronic boroles and even more powerful acids than trisarylgermylium and silylium ions (see Fig. 5).[16,20,36] The solid-state structures of **19**[OTf] and **20**[OTf] confirm their ionic constitution with clearly separated oxophosphonium cations and triflate anions (see ESI†). Overall, the metrics of the heterolyl ring of the cations [**19a**]$^+$, [**19b**]$^+$ and [**20**]$^+$ are very close to those of the covalent triflates **15** and **16** and the imidazolium cations [**17**]$^+$ and [**18**]$^+$. Fig. 3c shows as a representative example the molecular structure of [**19b**]$^+$. Attempts to measure the actual Lewis acidity of the covalent triflates **15** and **16** using the weaker nucleophilic *p*-fluorobenzonitrile (FBN method) failed due to their missing reactivity against nitriles.[63] Although the attempts to dissolve a sample of **15a** in THF resulted in the formation of a polymeric material, the covalent triflates **15** and **16** are only poor catalysts in the Diels Alder reaction (DAR) of 2,3-dimethylbutadiene with methylacrylate at room temperature. For example, 5 mol% of **15a** as catalyst gives after 4 d at room temperature a conversion of only 13% (see ESI for details†). $AlCl_3$, the standard catalyst for this type of DAR gives under the same conditions a marginal turn-over of 4%.

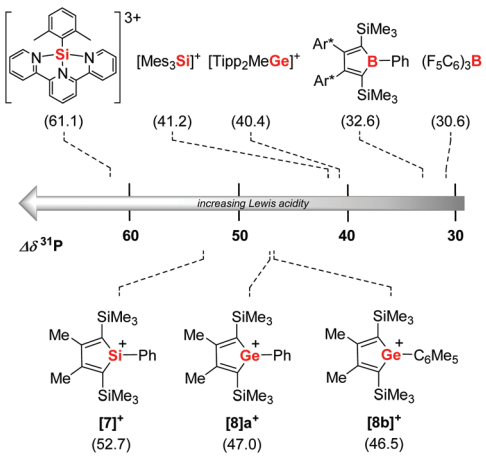

Fig. 5 Lewis acidity of germolyl [**8**]$^+$ and silolyl cations [**7**]$^+$ according to the Gutmann–Beckett scale and comparison with related main group element based Lewis acids (Ar* = 3,5-di-*t*-butylphenyl).[20,36,64,65]

Conclusions

Tetrolyl cations [**7**]$^+$ and [**8**]$^+$ are predicted to be antiaromatic compounds with Lewis acidities that are significantly higher than those determined for related boroles and predicted for alumoles. Established protocols for the synthesis of silylium and germylium ions failed in the case of tetrolyl cations [**7**]$^+$ and [**8**]$^+$. In contrast, the covalent tetrolyl triflates **15** and **16** are available in high yields from the corresponding chlorides by simple salt metathesis reactions. These are ideal starting materials for the preparation of ionic tetrolyl derivates. The reaction with the N-heterocylic carbene $ImMe_4$ gives access to tetrolylimidazolium ions [**17**]$^+$ and [**18**]$^+$. NMR spectroscopic and structural data of the ionic triflates [**17**]OTf and [**18**]OTf identifies them as typical imidazolium salts with no tetrolyl cation character. Consistently, the covalent triflates **15**, **16** show little activity as Lewis acids in Diels Alder cyclizations. The triflate substituent in **15** and **16** is replaced by triethylphosphane oxide to give the corresponding oxophosphonium salts [**19**]OTf and [**20**]OTf. Comparison of their ^{31}P NMR chemical shift with that of the free phosphane oxide confirms the high Lewis acidity of the underlying tetrolyl cations [**7**]$^+$ and [**8**]$^+$ (Gutmann–Beckett Lewis acidity scale). From a synthetic perspective, the covalent (**15**, **16**) and the ionic triflates [**17**]OTf–[**20**]OTf are useful reagents for the transfer of electrophilic silolyl or germolyl units.

Conflicts of interest

There are no conflicts to declare.

Acknowledgements

This work was supported by the DFG *via* the GRK 2226. Computations were done at the HPC Cluster, CARL, University of Oldenburg, funded by the DFG (INST 184/108-1 FUGG) and the Ministry of Science and Culture (MWK) of the Lower Saxony State.

Notes and references

1 M. Shimizu, *Main Group Strategies Funct. Hybrid Mater.*, 2017, 163–195, DOI: 10.1002/9781119235941.ch7.
2 S. Santra, *ChemistrySelect*, 2020, **5**, 9034–9058.
3 Y. Cai, A. Qin and B. Z. Tang, *J. Mater. Chem. C*, 2017, **5**, 7375–7389.
4 Y. Adachi and J. Ohshita, *Main Group Strategies Funct. Hybrid Mater.*, 2017, 237–264, DOI: 10.1002/9781119235941.ch10.
5 S. Yamaguchi and K. Tamao, *Bull. Chem. Soc. Jpn.*, 1996, **69**, 2327–2334.
6 S. Yamaguchi and K. Tamao, *J. Chem. Soc., Dalton Trans.*, 1998, 3693–3702, DOI: 10.1039/A804491K.

7 S. Yamaguchi, T. Endo, M. Uchida, T. Izumizawa, K. Furukawa and K. Tamao, *Chem. – Eur. J.*, 2000, **6**, 1683–1692.
8 A. V. Denisova, J. Tibbelin, R. Emanuelsson and H. Ottosson, *Molecules*, 2017, **22**, 370.
9 J. Luo, Z. Xie, J. W. Y. Lam, L. Cheng, H. Chen, C. Qiu, H. S. Kwok, X. Zhan, Y. Liu, D. Zhu and B. Z. Tang, *Chem. Commun.*, 2001, 1740–1741, DOI: **10.1039/B105159H**.
10 Z. Zhao, B. He and B. Z. Tang, *Chem. Sci.*, 2015, **6**, 5347–5365.
11 J. L. Mullin and H. J. Tracy, *Aggregation–Induced Emission: Fundamentals and Applications*, Vol. 1 and 2, 2013, 39–60. DOI: **10.1002/9781118735183.ch02**.
12 Z. Dong, L. Albers and T. Müller, *Acc. Chem. Res.*, 2020, **53**, 532–543.
13 C. R. W. Reinhold, M. Schmidtmann, B. Tumanskii and T. Müller, *Chem. – Eur. J.*, 2021, **27**, 12063–12068.
14 Z. Dong, M. Schmidtmann and T. Müller, *Chem. – Eur. J.*, 2019, **25**, 10858–10865.
15 Z. Dong, C. R. W. Reinhold, M. Schmidtmann and T. Müller, *Organometallics*, 2018, **37**, 4736–4743.
16 T. Heitkemper and C. P. Sindlinger, *Chem. – Eur. J.*, 2020, **26**, 11684–11689.
17 H. Braunschweig, I. Fernández, G. Frenking and T. Kupfer, *Angew. Chem., Int. Ed.*, 2008, **47**, 1951–1954.
18 J. Köhler, S. Lindenmeier, I. Fischer, H. Braunschweig, T. Kupfer, D. Gamon and C.-W. Chiu, *J. Raman Spectrosc.*, 2010, **41**, 636–641.
19 A. Iida, A. Sekioka and S. Yamaguchi, *Chem. Sci.*, 2012, **3**, 1461–1466.
20 T. Heitkemper, L. Naß and C. P. Sindlinger, *Dalton Trans.*, 2020, **49**, 2706–2714.
21 C.-W. So, D. Watanabe, A. Wakamiya and S. Yamaguchi, *Organometallics*, 2008, **27**, 3496–3501.
22 T. Agou, T. Wasano, P. Jin, S. Nagase and N. Tokitoh, *Angew. Chem., Int. Ed.*, 2013, **52**, 10031–10034.
23 T. Agou, T. Wasano, T. Sasamori and N. Tokitoh, *Organometallics*, 2014, **33**, 6963–6966.
24 T. Wasano, T. Agou, T. Sasamori and N. Tokitoh, *Chem. Commun.*, 2014, **50**, 8148–8150.
25 R. Drescher, B. Ritschel, R. D. Dewhurst, A. Deißenberger, A. Hofmann and H. Braunschweig, *Chem. Commun.*, 2021, **57**, 7505–7508.
26 V. Y. Lee, H. Sugasawa, O. A. Gapurenko, R. M. Minyaev, V. I. Minkin, H. Gornitzka and A. Sekiguchi, *Organometallics*, 2022, **41**, 467–471.
27 K. Huynh, J. Vignolle and T. D. Tilley, *Angew. Chem., Int. Ed.*, 2009, **48**, 2835–2837.
28 C. Fan, W. E. Piers and M. Parvez, *Angew. Chem., Int. Ed.*, 2009, **48**, 2955–2958.
29 C. Fan, L. G. Mercier, W. E. Piers, H. M. Tuononen and M. Parvez, *J. Am. Chem. Soc.*, 2010, **132**, 9604–9606.
30 C. Fan, W. E. Piers, M. Parvez and R. McDonald, *Organometallics*, 2010, **29**, 5132–5139.
31 A. Fukazawa, J. L. Dutton, C. Fan, L. G. Mercier, A. Y. Houghton, Q. Wu, W. E. Piers and M. Parvez, *Chem. Sci.*, 2012, **3**, 1814–1818.
32 The computations were performed with the Gaussian-16 program, see the ESI material for details.†
33 Z. Chen, C. S. Wannere, C. Corminboeuf, R. Puchta and P. V. R. Schleyer, *Chem. Rev.*, 2005, **105**, 3842–3888.
34 A. Stanger, *J. Org. Chem.*, 2006, **71**, 883–893.
35 M. T. Mock, R. G. Potter, D. M. Camaioni, J. Li, W. G. Dougherty, W. S. Kassel, B. Twamley and D. L. DuBois, *J. Am. Chem. Soc.*, 2009, **131**, 14454–14465.
36 H. Großekappenberg, M. Reißmann, M. Schmidtmann and T. Müller, *Organometallics*, 2015, **34**, 4952–4958.
37 H. F. T. Klare, L. Albers, L. Süsse, S. Keess, T. Müller and M. Oestreich, *Chem. Rev.*, 2021, **121**, 5889–5985.
38 J. Y. Corey and R. West, *J. Am. Chem. Soc.*, 1963, **85**, 2430–2433.
39 J. Y. Corey, *J. Am. Chem. Soc.*, 1975, **97**, 3237–3238.
40 J. B. Lambert, Y. Zhao, H. Wu, W. C. Tse and B. Kuhlmann, *J. Am. Chem. Soc.*, 1999, **121**, 5001–5008.
41 Y. Ishida, A. Sekiguchi and Y. Kabe, *J. Am. Chem. Soc.*, 2003, **125**, 11468–11469.
42 C. Schenk, C. Drost and A. Schnepf, *Dalton Trans.*, 2009, 773–776, DOI: **10.1039/B818931E**.
43 N. Kuhn, T. Kratz, D. Bläser and R. Boese, *Chem. Ber.*, 1995, **128**, 245–250.
44 D. Mendoza-Espinosa, B. Donnadieu and G. Bertrand, *J. Am. Chem. Soc.*, 2010, **132**, 7264–7265.
45 J. J. Weigand, K.-O. Feldmann and F. D. Henne, *J. Am. Chem. Soc.*, 2010, **132**, 16321–16323.
46 M. F. Silva Valverde, E. Theuergarten, T. Bannenberg, M. Freytag, P. G. Jones and M. Tamm, *Dalton Trans.*, 2015, **44**, 9400–9408.
47 V. Nesterov, D. Reiter, P. Bag, P. Frisch, R. Holzner, A. Porzelt and S. Inoue, *Chem. Rev.*, 2018, **118**, 9678–9842.
48 A. J. Arduengo, H. V. R. Dias, R. L. Harlow and M. Kline, *J. Am. Chem. Soc.*, 1992, **114**, 5530–5534.
49 K. M. Baines and W. G. Stibbs, *Coord. Chem. Rev.*, 1995, **145**, 157–200.
50 M. Kaftory, M. Kapon and M. Botoshansky, in *The Chemistry of Organic Silicon Compounds*, eds Z. Rappoport and Y. Apeloig, Wiley, Chichester UK, 1998, vol. 2, pp. 181–265.
51 P. A. Rupar, M. C. Jennings, P. J. Ragogna and K. M. Baines, *Organometallics*, 2007, **26**, 4109–4111.
52 P. A. Rupar, M. C. Jennings and K. M. Baines, *Organometallics*, 2008, **27**, 5043–5051.
53 A. J. Ruddy, P. A. Rupar, K. J. Bladek, C. J. Allan, J. C. Avery and K. M. Baines, *Organometallics*, 2010, **29**, 1362–1367.
54 Z. Xie, R. Bau, A. Benesi and C. A. Reed, *Organometallics*, 1995, **14**, 3933–3941.
55 Z. Xie, J. Manning, R. W. Reed, R. Mathur, P. D. W. Boyd, A. Benesi and C. A. Reed, *J. Am. Chem. Soc.*, 1996, **118**, 2922–2928.
56 R. Becerra and R. Walsh, in *The Chemistry of Organosilicon Compounds*, ed. Z. Rappoport and Y. Apeloig, John Wiley & Sons, 1998, vol. 2, p. 153.
57 R. Becerra and R. Walsh, in *Organosilicon Compounds*, ed. V. Y. Lee, Elsevier, 2017, p. 79.
58 R. Becerra and R. Walsh, *Phys. Chem. Chem. Phys.*, 2019, **21**, 988–1008.

59 J. H. Wright, G. W. Mueck, F. S. Tham and C. A. Reed, *Organometallics*, 2010, **29**, 4066–4070.
60 M. Talavera, G. Meißner, S. G. Rachor and T. Braun, *Chem. Commun.*, 2020, **56**, 4452–4455.
61 U. Mayer, V. Gutmann and W. Gerger, *Monatsh. Chem.*, 1975, **106**, 1235–1257.
62 M. A. Beckett, G. C. Strickland, J. R. Holland and K. Sukumar Varma, *Polymer*, 1996, **37**, 4629–4631.
63 S. Künzler, S. Rathjen, A. Merk, M. Schmidtmann and T. Müller, *Chem. – Eur. J.*, 2019, **25**, 15123–15130.
64 A. Hermannsdorfer and M. Driess, *Angew. Chem., Int. Ed.*, 2020, **59**, 23132–23136.
65 M. A. Beckett, D. S. Brassington, S. J. Coles and M. B. Hursthouse, *Inorg. Chem. Commun.*, 2000, **3**, 530–533.